Simplification of Non-linear Dynamic Design Procedure on Steel Moment-resisting Frames to Seismic Actions

by
ITO Takumi [I], OHI Kenichi [II], KHANDELWAL Praveen [I]

Abstract

To simplify the non-linear dynamic design procedure on steel moment-resisting frames to seismic actions, a new design-friendly reduced analysis method is proposed: Global safety domain against plastic collapse of an elastic-plastic frame becomes a convex polyhedron, and its whole figure is approximated also by a hyper-ellipsoidal yield surface from a few reference points on the surface. Normality rule of plastic velocity on the surface and elasticity inside the hyper-ellipsoid are assumed to trace the global restoring force of the frame in the proposed method, and also higher modal components of restoring force are ignored to reduce the number of degree-of-freedoms. Its validity is checked by comparison with the results of member-hysteresis based full-mode analysis.

1. Introduction

The emphasis in seismic resistance design is shifting from 'strength' to 'performance' following the demand and collapse of numerous structures during recent earthquake. Gradually, performance based designs are becoming a part of code provisions with publication of FEMA-273[1] in USA and Enforcement Order and Regulation after Building Standard Law of Japan was revised in 1998[2]. At the same time, it may be fair to say that simple and efficient methods for capturing the essential/important features affecting the performance have not been adequately developed. The objective of this paper is to develop a design friendly method for performance evaluation of ductile steel moment resisting frames, which are used as the primary lateral load resisting systems in many middle-rise buildings. Proposed research focuses on the simplifications of nonlinear dynamic procedures (NDP). This study intends to benefit the design engineer by bringing NDP, which is usually considered complicated and costly, within the reach of a structural engineer, who is familiar with linear dynamic analysis.

This paper presents a nonlinear dynamic procedure with partial-mode response analysis with simplified plastic failure surface model. A safety domain about plastic collapse of an elastic-perfectly plastic frame is approximated by a yield-polyhedron with a reduced number of failure mechanisms. To reduce the number of failure mechanisms, a preliminary analysis based on FOSM reliability method is proposed by the authors[3][4]. This method requires, however, an exhaustive procedure to enumerate the whole failure mechanisms, and the failure surface becomes a convex polyhedron made of a lot of hyper surfaces even after they are reduced. Sometimes it happens to encounter the problem of dealing with extreme points during the renewal procedure of restoring force. To avoid them, an alternative method is proposed in this paper. The plastic failure surface is approximated by a hyper-ellipsoidal model, which has no extreme point and provides a much easier procedure to trace the inelastic global behavior than the yield polyhedron model. Additionally, the method proposed does not require the enumeration of enormous failure mechanisms to arrange the hyper-ellipsoid.

I) Doctor Candidate, Graduate School of Engineering, University of Tokyo
II) Associate Professor, Institute of Industrial Science, University of Tokyo

2. Analytical method

2.1 Transformation of coordinates

The equation of motion for a multi-degree-of-freedom system with viscous damping and hysteresis inelastic restoring force under seismic excitation is represented as:

$$[M]\cdot\{\ddot{x}\}+[C]\cdot\{\dot{x}\}+\{f\}=-[M]\cdot\{1\}\cdot\ddot{y} \tag{1}$$

where $[M]$ is mass matrix, $[C]$ is damping matrix, $\{x\}$ is displacement vector relative to the ground, $\{f\}$ is restoring force vector, and $\ddot{y}$ is the ground acceleration.

Here we define the transformation of displacement and restoring force into modal coordinates as:

Transformation of displacement: $\{x\}=[\phi]\cdot\{q\}$ (2)

Transformation of restoring force: $\{f\}=\left[\phi^T\right]^{-1}\cdot\{r\}=[\Psi]\cdot\{r\}$ (3)

where $\{q\}$ is modal displacement vector, $\{r\}$ is modal restoring force vector, $[\phi]$ is modal participation matrix, and $\{\psi_j\}$ is the j-th base vector for force given as a column vector of $[\Psi]=\left[\phi^T\right]^{-1}$.

By this transformation the equation of motion on the modal space is given by:

$$\ddot{q}+2\cdot h_j\cdot\omega_j\cdot\dot{q}_j+r_j/m^*_j=-\ddot{y} \tag{4}$$

where h_j is the j-th modal damping constant, ω_j is the j-th natural circular frequency.

2.2 The calculation of modal displacement increment

The modal displacement increment can be calculated based on explicit numerical integration (central finite difference) from the j-th modal component of restoring force:

$$\Delta q_j^{(k+1)}=\frac{\left(1-h_j\omega_j\Delta t\right)}{\left(1+h_j\omega_j\Delta t\right)}\Delta q_j^{(k)}-\frac{\Delta t^2}{\left(1+h_j\omega_j\Delta t\right)}\left(\frac{r_j^{(k)}}{m_j^*}+\ddot{y}^{(k)}\right) \tag{5}$$

where $\Delta q_j^{(k+1)}=q_j^{(k+1)}-q_j^{(k)}$

2.3 Reduced yield polyhedron model [3] [4]

A simple proposal to calculate global inelastic responses of MDOF steel moment resisting frames was made by the authors [3][4], where a global yield surface model of a frame was arranged and simplified based on the limit analysis and the first-order reliability method (FORM). First, a procedure was proposed for 'vibration mode-failure mode' integrated analysis, wherein the restoring force characteristics are represented by a global convex yield polyhedron model, instead of a set of member hysteresis based models usually adopted in the inelastic structural analysis. Then FORM is extended to seismic design in the form of 'random pushover analysis', to choose an appropriate number of failure mechanisms to be considered in the analysis.

(1) Equivalent-Static Seismic Loading Model

A simple equivalent-static seismic loading model is adopted only in the preliminary analysis to choose important failure mechanisms. As the ground motion varies randomly in time, mean value or expected value of modal restoring forces is taken as zero, and the vibration modes are considered independent. In an usual notation of $E()$ for expected value:

$$E(r_j)=\bar{r}_j=0\ ;\ E(r_i r_j)=0\quad(i\neq j) \tag{6}$$

$$\sigma_{rj} = c \cdot m^*{}_j \cdot S_{aj} \tag{7}$$

where r_j is the j-th modal restoring force, $m^*{}_j$ is the j-th effective mass, σ_{rj} is standard deviation of the modal restoring force, c is a constant which is determined from the relationship between the standard deviation of modal restoring force at arbitrary points in time and its mean extreme and is taken tentatively as one-third for all the vibration modes [5] [6], S_{aj} is ordinate of acceleration response spectra, which depends on natural period and damping of j-th vibration mode.

(2) Reduction of Failure Mechanisms

Stochastic limit analysis, based on FORM, is applied for identification of more likely failure mechanisms. It is assumed that the seismic action and the resistance are independent of each other. The performance or limit state function denoted by g corresponding to each failure mechanism can be written in terms of the energy dissipated by plastic portions and the work done by seismic action as:

$$g = \sum_{i=1}^{m} M_{pi} \cdot \left|\theta_{pi}\right| - \sum_{j=1}^{n} a_j \cdot r_j \tag{8}$$

where m is number of plastic portions (plastic hinges) and n is number of vibration modes. The energy dissipated by plastic portions is represented by $\sum_{i=1}^{m} M_{pi} \cdot \left|\theta_{pi}\right|$, where M_{pi} is the basic variable of element moment capacity and $\left|\theta_{pi}\right|$ denotes the rotation of the corresponding plastic hinge. The work done by the seismic action is expressed in the modal coordinates and represented by $\sum_{j=1}^{n} a_j \cdot r_j$, where a_j is the j-th modal component of plastic deformation compatible with the before-mentioned plastic hinge rotations.

Mean value of g: $$\mu_g = \sum_{i=1}^{m} \overline{M}_{pi} \cdot \left|\theta_{pi}\right| - \sum_{j=1}^{n} a_j \cdot \overline{r}_j \tag{9}$$

Standard deviation: $$\sigma_g = \sqrt{\sum_{i=1}^{m} \sigma_{mpi}{}^2 \cdot \theta_{pi}{}^2 + \sum_{j=1}^{n} (\sigma_{rj})^2 \cdot (a_j)^2} \tag{10}$$

where $\overline{M}_{pi}$, $\overline{r}_j$ are mean values, and σ_{mpi}, σ_{rj} are standard deviations of resistance capacity and load, respectively.

As the mean values of seismic action is taken zero if we adopt the equivalent-static model in the previous section, the FOSM reliability index, denoted by β, corresponding to the mechanism failure is given by:

Reliability index: $$\beta = \frac{\mu_g}{\sigma_g} = \sum_{i=1}^{m} \overline{M}_{pi} \cdot \left|\theta_{pi}\right| \Big/ \sigma_g \tag{11}$$

A lower reliability index indicates higher probability of failure. In our view, failure mechanisms with probability less than about 10% of the most likely ($\beta_{\min}$) failure mechanism can be excluded from further analysis. Alternatively, failure mechanisms with $\beta \geq \beta_{\min} + \Delta$ can be neglected. In case of a normal distribution and if $\beta_{\min} \geq 1.4$, Δ equal to unity would be adequate. In addition, the maximum number of failure mechanisms considered should preferably be limited to the number of vibration degrees of freedom, to avoid possibility of ill conditioning during dynamic analysis.

For structures with very large numbers of potential failure mechanisms, mutual correlation between the failure mechanisms should be considered, as many of them may be partially correlated. PNET [7], which stands for probabilistic network evaluation technique, can be applied for such a situation. The correlation coefficient between the two failure modes a and b, whose performance functions are denoted by $g_a = \sum_{i=1}^{m} M_{api} \cdot \left|\theta_{api}\right| - \sum_{j=1}^{n} a_j \cdot r_j$, $g_b = \sum_{i=1}^{m} M_{bpi} \cdot \left|\theta_{bpi}\right| - \sum_{j=1}^{n} a_j \cdot r_j$ respectively, can be written as:

$$\rho_{ab} = \frac{E[(g_a - E(a_a))\cdot(g_b - E(a_b))]}{\sigma_{ag}\cdot\sigma_{bg}} \tag{12}$$

where σ_{ag}, σ_{bg} are standard deviation of g_a, g_b respectively, and if we ignore the uncertainty of moment capacities, they can be written as:

$$\rho_{ab} = \frac{\sum_{j=1}^{n} a_j \cdot b_j \cdot \sigma_{rj}^{\,2}}{\sqrt{\sum_{j=1}^{n} a_j \cdot \sigma_{rj}^{\,2} \cdot \sum_{j=1}^{n} b_j \cdot \sigma_{rj}^{\,2}}} \tag{13}$$

Failure mechanisms with correlation coefficients more than a demarcating correlation are unified and represented by a single failure mechanism having lowest reliability index among them.

2.4 Ellipsoidal yield surface model

Another much simpler approach is proposed by use of an ellipsoidal approximation of global safety domain against plastic collapse. From general view of exact safety domain, an ellipsoidal body can outline a convex figure of exact yield polyhedron. Such a hyper-ellipsoid in n-dimensional force space can be determined so that it shares different $n(n+1)/2$ reference points on the exact yield surface. Then pushover limit analysis on a frame under $n(n+1)/2$ different load patterns is performed to obtain these reference points, and the safety domain is approximated by an n-dimensional hyper-ellipsoidal body.

(1) Pushover Limit Analysis to Obtain Reference Points on Yield Surface

On the limit analysis of the frames, the following problem is solved:

Maximize λ (14)

Subject to Equilibrium equation $\lambda\cdot\{P_0\} = [\ \ Con\ \ ]\cdot\{M\}$ (15)

Plastic condition $|M_i| \le M_{pi}$ (15')

where λ is load factor, $\{P_0\}$ is load pattern vector, $[Con]$ is connectivity matrix, $\{M\}$ is element moment vector, M_{pi} is element moment capacity of M_i.

It is convenient to represent the load pattern vector as a linear combination of modal load patterns corresponding to elastic seismic load effect as adopted in the previous sections. In a general form, it is expressed by:

$$\lambda\{P_0\} = [\phi^T]^{-1}\cdot\{r\} = [\Psi]\cdot\{r\} = r_1\cdot\{\psi_1\} + r_2\cdot\{\psi_2\} + \cdots + r_n\cdot\{\psi_n\} \tag{16}$$

If we choose two dominant load patterns denoted by $\{\psi_i\}$ and $\{\psi_j\}$ instead of considering all the vibration modes, and if we consider the ratio of dominancy based on the magnitude of elastic seismic load effect, then a simplified load pattern may take the following form:

$$\lambda\cdot\{P_0\} = \lambda\cdot\{\psi_i\} \pm \lambda\cdot\alpha_{ij}\cdot\{\psi_j\} \tag{17}$$

where $|\alpha_{ij}| = m^*_j\cdot S_a(T_j)/m^*_i\cdot S_a(T_i)$

The combination of i and j is determined as follows:

An ellipsoid in n-dimensional force space can be determined so that it shares different $n(n+1)/2$ reference points on the exact yield surface. Then pushover limit analysis on a frame under $n(n+1)/2$ different load patterns is performed to obtain these reference points.

First, $n \times n$ square formation is prepared, it is better to arrange as the parameter with high probability of occurrence appears many times. And then, the group of load pattern is determined as illustrated in Fig.1 because there are n $(n+1)/2$

combinations at the upper left triangular potions in the $n \times n$ square formation.

After the load pattern is determined, the limit analysis of the structure is performed to obtain the reference points. These reference points are supposed to satisfy the following equation:

$$\{r^*\}_k^T \cdot [A] \cdot \{r^*\}_k = 1 \quad k = 1, \cdots, n \cdot (n+1)/2 \tag{18}$$

where *[A]* is a symmetrical matrix that controls the shape and the inclination of the n-th dimensional hyper-ellipsoid. The number of indeterminate components of matrix *[A]* is $n(n+1)/2$, and then they can be determined by solving the simultaneous equation (18).

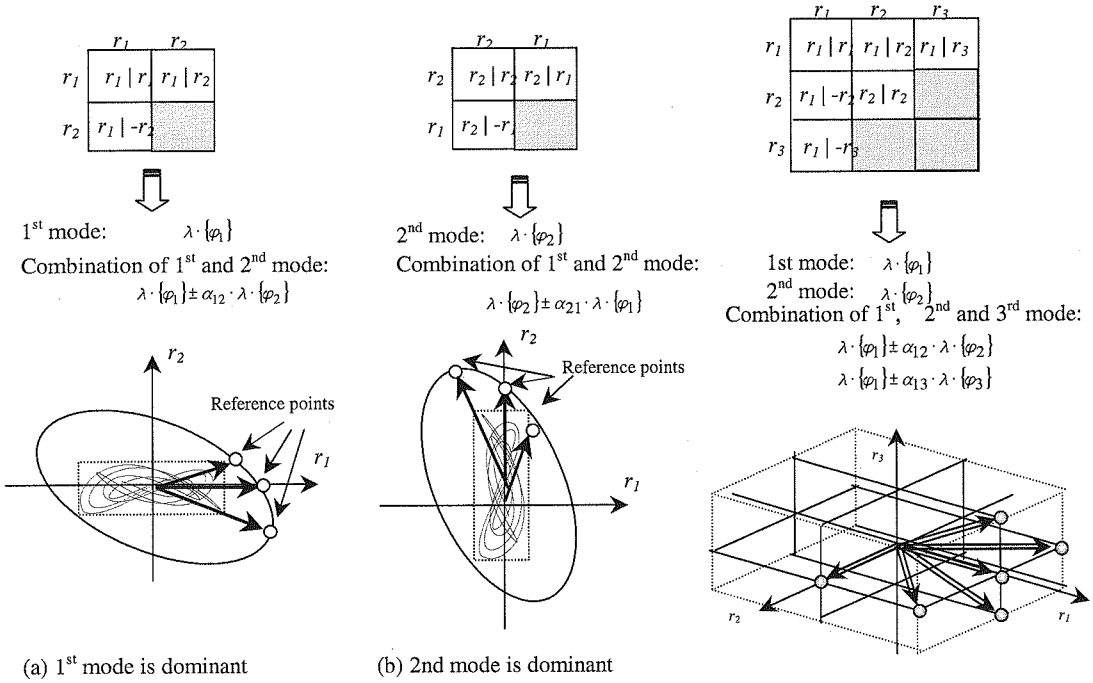

(a) 1st mode is dominant (b) 2nd mode is dominant

The case of two-degree of freedom **The case of three-degree of freedom**

Fig.1 Load pattern selection used in preliminary pushover limit analysis

(2) Tracing of restoring force Point

The modal displacement increment is applied to the frame, and inelastic restoring force is traced and renewed in the following manner. There are two methods possible to trace and renew the restoring force: The first is that the restoring force is traced on the full-mode restoring force space while the partial-mode technique is used for the integration of equation of motion, and the second is that the tracing of restoring force and the integration of equation of motion are both performed on the partial-mode restoring force space. The latter handling is easier and adopted herein.

Now the intersection of ellipsoidal yield surface model on the partial-mode restoring force space is denoted by $\{\tilde{r}\}^T \cdot [A] \cdot \{\tilde{r}\} = 1$. After modal displacement increment is obtained by central difference method, modal restoring force increment is calculated by assuming that the structure remains in elastic range as:

$$\{\Delta \tilde{r}_e\} = [\tilde{K}_e] \cdot \{\Delta \tilde{q}\} \tag{19}$$

where $[\tilde{K}_e]$ is modal generalized stiffness matrix given by $[\tilde{K}_e]=Diag[k_j^*]$ as $k_i^* = \{\phi_j\}^T \cdot [K] \cdot \{\phi_j\}$.

If the structure would remain in elastic range, the new modal restoring force would be given by:

$$\{\tilde{r}_{new}\}=\{\tilde{r}^{(k)}\}+\{\Delta\tilde{r}_e\} \tag{20}$$

And then, it is judged by the following equation whether the new location of modal restoring force is inside the hyper-ellipsoid or outside:

$$\{\tilde{r}_{new}\}^T \cdot [\tilde{A}] \cdot \{r_{new}\} \le 1 \quad \text{(Inside of hyper-ellipsoid)} \tag{21a}$$

$$\{\tilde{r}_{new}\}^T \cdot [\tilde{A}] \cdot \{\tilde{r}_{new}\} > 1 \quad \text{(Outside of hyper-ellipsoid)} \tag{21b}$$

If the location is inside the hyper-ellipsoid, the modal restoring force at next step is given by $\{\tilde{r}^{(k+1)}\}=\{\tilde{r}_{new}\}$. But if the location is thrown over the hyper-ellipsoid, the following modification of modal restoring force is carried out:

The intersection of path and the hyper-ellipsoidal yield surface is denoted by $\{\tilde{r}_{cross}\}$,

$$\{\tilde{r}_{cross}\}=\{\tilde{r}^{(k)}\}+\tau \cdot \{\Delta\tilde{r}_e\} \tag{22}$$

where $\tau=\dfrac{-\tau_1+\sqrt{\tau_1^2+\tau_2\cdot(1-\tau_3)}}{\tau_2}$, $\tau_1=\{\Delta\tilde{r}_e\}^T \cdot [\tilde{A}] \cdot \{\tilde{r}^{(k)}\}$, $\tau_2=\{\Delta\tilde{r}_e\}^T \cdot [\tilde{A}] \cdot \{\Delta\tilde{r}_e\}$, $\tau_3=\{\tilde{r}^{(k)}\}^T \cdot [\tilde{A}] \cdot \{\tilde{r}^{(k)}\}$.

Next the plastic displacement increment $\{\Delta\tilde{q}_p\}$ is assumed to follow the flow rule or normality rule. $\{\Delta\tilde{q}_p\}$ is given by $\gamma \cdot [\tilde{A}] \cdot \{\tilde{r}_{cross}\}$ if a normal direction is represented at $\{\tilde{r}_{cross}\}$. Then the restoring force at next step $\{\tilde{r}^{(k+1)}\}$ satisfies the following equation including an indeterminate factor:

$$\begin{aligned}\{\tilde{r}^{(k+1)}\} &= \{\tilde{r}^{(k)}\}+[\tilde{K}_e]\cdot\{\Delta\tilde{q}_e\}\\ &= \{\tilde{r}^{(k)}\}+[\tilde{K}_e]\cdot\{\Delta\tilde{q}-\Delta\tilde{q}_p\}\\ &= \{\tilde{r}_{new}\}-\gamma\cdot[\tilde{K}_e]\cdot[\tilde{A}]\cdot\{\tilde{r}_{cross}\}\\ &= \{\tilde{r}_{new}\}-\gamma\cdot\{\tilde{h}_{pull}\}\end{aligned} \tag{23}$$

where $\{\tilde{h}_{pull}\}=[\tilde{K}_e]\cdot[\tilde{A}]\cdot\{\tilde{r}_{cross}\}$.

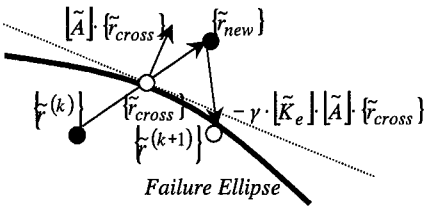

Fig. 2 Renewal of modal restoring force

The indeterminate factor γ is solved from the condition that $\{\tilde{r}^{(k+1)}\}$ lies on the surface of the hyper-ellipsoid.

$$\gamma=\frac{\gamma_1-\sqrt{\gamma_1^2-\gamma_2\cdot(\gamma_3-1)}}{\gamma_2} \tag{24}$$

where γ_1, γ_2, and γ_3 are given by $\gamma_1=\{\tilde{r}_{new}\}^T\cdot[\tilde{A}]\cdot\{\tilde{h}_{pull}\}$, $\gamma_2=\{\tilde{h}_{pull}\}^T\cdot[\tilde{A}]\cdot\{\tilde{h}_{pull}\}$, and $\gamma_3=\{\tilde{r}_{new}\}^T\cdot[\tilde{A}]\cdot\{\tilde{r}_{new}\}$, respectively.

3. Examples

3.1 Yield polyhedron model

(1) An Illustrative Example of Two-story Single-bay Frame

A two-story single-bay frame as shown in Fig. 3 is taken to study basic principles of yield polyhedron. The ratio of span

(L) to storey height (H) and mass at 2nd floor to roof are 1.6 and 1.5464, respectively. The total weight (W) of the frame is 484 kN. 2% modal damping is assumed for both vibration modes. The elastic natural periods for the first and the second mode are 1.23 and 0.472 seconds, respectively. The frame is analysed for El Centro (NS) 1940 ground motion with the peak ground acceleration scaled to 0.3m/sec^2. The failure modes possible in this situation are shown in Fig. 4.

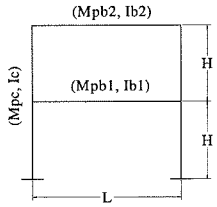

Fig. 3 Two Story Single Bay Frame

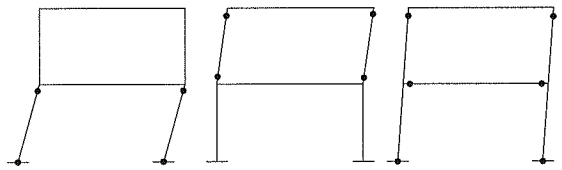

1st Story Local Collapse 2nd Story Local Collapse Combined Mechanism

Fig. 4 - Failure Modes of the two-story frame

The response of the structure in terms of restoring force is confined within a convex region bounded on all sides by the failure planes. Fig. 5 shows such a yield polyhedron for the two-story frame. The f_1 and f_2 represent the restoring forces (in original space) at the second floor and roof level, respectively. Representation of the restoring force characteristics of the structure by a yield polyhedron model considerably reduces the size of the analysis, compared with member-hysteresis based models usually employed in the inelastic frame analysis. The likely failure mechanisms can be drawn based on the experience, or the stochastic limit analysis using compact procedure [8] [9] may be used for complex situations. Sequence of yielding before a mechanism formation i.e. partial yielding is ignored in the yield polyhedron model. The locus of restoring forces can move within or tangentially on the boundary of the yield polyhedron, as shown in Fig. 6 for the two-story frame.

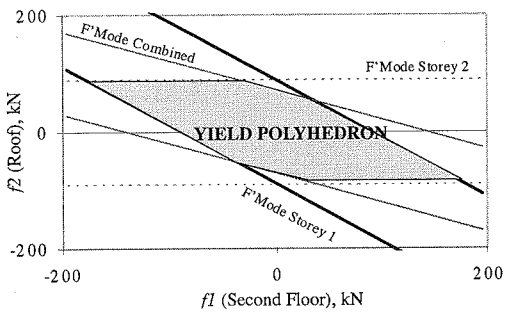

Fig. 5 Global Yield Polyhedron in Original Restoring Force Space

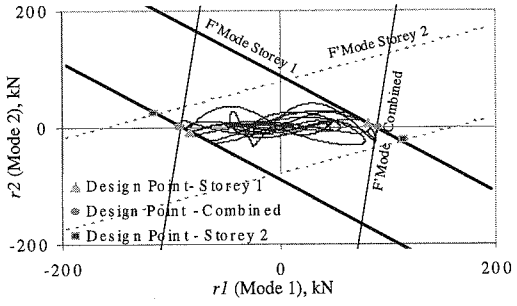

Fig. 6 Locus of Restoring Force and Design Points in Modal Space

(2) Reduced yield polyhedron model for six-story two-bay frame

A six-story two-bay frame shown in Fig. 7 is studied hereafter. The storey height is 3.75 m and span of each bay is 6 m. The member properties and floor weights are shown in Table 1 and 2, respectively. The modulus of elasticity and yield stress for steel is taken as 205 GPa and 235 MPa, respectively. A constant modal-damping ratio of 2% of critical damping is considered for all the vibration modes. The vibration periods are shown in Table 3. This frame is analysed for El Centro (NS), Hachinohe (EW), Fukiai (NS) ground motions and an impulse equivalent to 0.75 m/sec initial velocity. The details of the ground motions are shown in Table 4. The impulse level is selected from consideration of similar order of deformation pattern in comparison with other ground motions. The energy input spectra and acceleration response spectra are shown in Figs. 9 and 10, respectively.

As mentioned in the previous section, a set of failure mechanisms with correlation coefficient more than a demarcating correlation ρ_0 can be unified. In an ordinary reliability analysis involved with a failure probability range from 10^{-1} to 10^{-3}, a standard value $\rho_0 = 0.70$ is said to be appropriate [7]. Adoption of such a low value for the present purpose, however, resulted in the elimination of the majority of the failure modes for the six-story frame studied herein.

And then, a relatively high value of ρ_0 =0.97 was found to give satisfactory result. Tables 5 and 6 list the reliability indices of the failure mechanisms for the two-story frame in the previous section and the six-story frame, respectively. Table 7 lists the failure mechanisms obtained by PNET for the six-story frame.

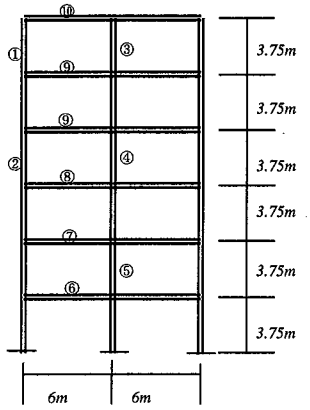

Fig. 7 Six-story Two-bay frame

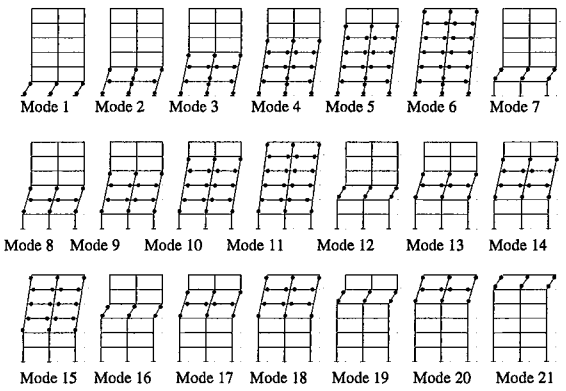

Fig. 8 Collapse Modes for six-story two-bay frame under lateral loading

Table 1. Member Properties

Member ID (Fig.7○)	Moment of Inertia ($10^{-8}m^4$)	Plastic Moment Capacity (kN.m)
1	2490	83.2
2	8090	194
3	5700	151
4	11300	247
5	14900	302
6	23100	307
7	16300	239
8	11800	189
9	8360	148
10	3890	86.3

Table 2. Floor Weights

Floor	Weight (kN)
Roof	380
6	589
5	589
4	589
3	589
2	589

Table 3. Vibration Period (sec)

Mode	Time Period
1	2.57
2	0.98
3	0.57
4	0.43
5	0.31
6	0.23

The failure modes considered under horizontal loads are shown in Fig. 11 and have been drawn based on the experience. These include local story collapse mechanisms and combined mechanisms. Locations of the plastic hinges are assumed at the top and bottom ends of the columns, which have undergone side sway, and at the floor beams end connected with the side columns. At the junction of the floor beams and the central column, plastic hinges are assumed in the beams or in the columns, whichever is having the least summation of the plastic moment capacities at the junction.

Yield polyhedron approach enables a quick examination of the seismic response in terms of the failure modes of the structure, which is quite informative and helpful in understanding critical/ important design situations and in taking remedial measures.

Table 4 – Details of Ground Motions

Ground Motion	Earthquake	Peak Ground Acceleration (in gravity acceleration)	Duration (Sec)
El Centro (NS)	Imperial Valley, 1940	0.325	10
Hachinohe (EW)	Tokachi - Oki, 1968	0.186	30
Fukiai (NS)	Hyogoken –Nanbu, 1995	0.700	20

Table 5 Reliability Indices for Failure Mechanisms of Six-story Frame

Failure Mode	Reliability Index β			
	El Centro	Hachi-nohe	Fukiai	Impulse
1	1.912	1.232	1.439	2.026
2	1.943	1.204	1.450	2.080
3	1.939	1.152	1.437	2.034
4	1.986	1.142	1.475	2.037
5	1.955	1.102	1.455	1.977
6	2.110	1.184	1.574	2.127
7	2.189	1.324	1.618	2.261
8	2.020	1.178	1.498	2.063
9	2.011	1.147	1.505	2.036
10	1.865	1.051	1.395	1.878
11	2.054	1.156	1.530	2.070
12	2.392	1.398	1.799	2.367
13	2.107	1.228	1.609	2.129
14	1.803	1.050	1.358	1.851
15	2.027	1.186	1.505	2.098
16	2.715	1.668	2.088	2.723
17	1.861	1.154	1.387	1.982
18	2.097	1.324	1.539	2.288
19	1.560	1.057	1.138	1.712
20	1.911	1.360	1.416	2.230
21	2.273	1.982	1.835	2.623

Table 6 Reliability Indices for Failure Mechanisms of Two-story Frame

Failure Mode	Reliability Index
First Story	1.67
Second Story	2.68
Combined	1.79

Table 7 Failure Mechanisms by PNET for Six-story Frame

Seismic Motion	Failure Modes
El Centro	19,14,17,10,20,1
Hachinohe	14,19,5,3,2,21
Fukiai	19,14,17,10,3,1
Impulse	19,14,5,17,1,8

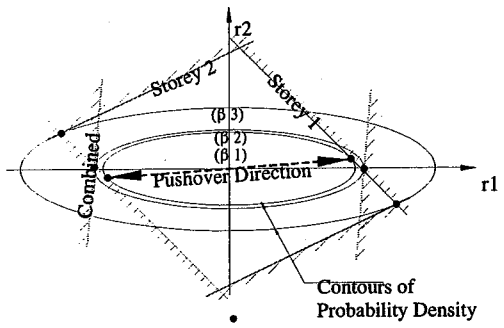

Fig.11 Design Point of Failure Modes

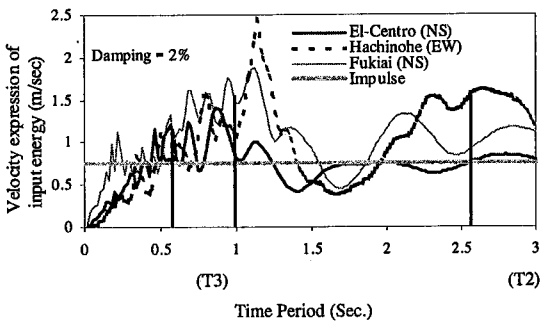

Fig. 9 Energy Input Spectra (in velocity expression)

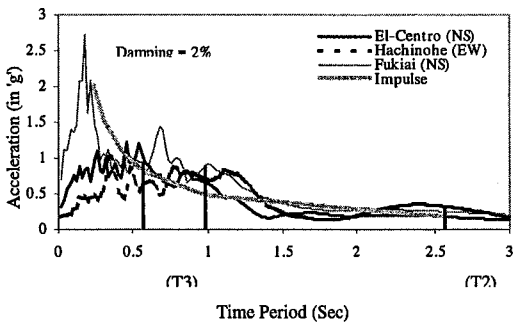

Fig. 10 Acceleration Response Spectra

(3) Response analysis with reduced yield polyhedron model

The six-story frame is analysed for El Centro (NS), Hachinohe (EW), Fukiai (NS) ground motions and an impulse of 0.75 m/sec velocity, by the proposed methods, referred to as RA To confirm the validity of RA, results have been compared with a member hysteresis based analysis, performed using a computer program DIANA [10] with all members being idealised as elastic-perfectly plastic. As there is vast amount of data, response histories of the top storey, the bottom storey and the most damaged storey i.e. fifth have shown for comparison. Fig. 12 shows the response histories of the storey drifts. Peak response values and time variations are well simulated. Fig. 13 compares the hysteresis loops of the storey shear v/s storey drifts. RA provides close approximations to DIANA.

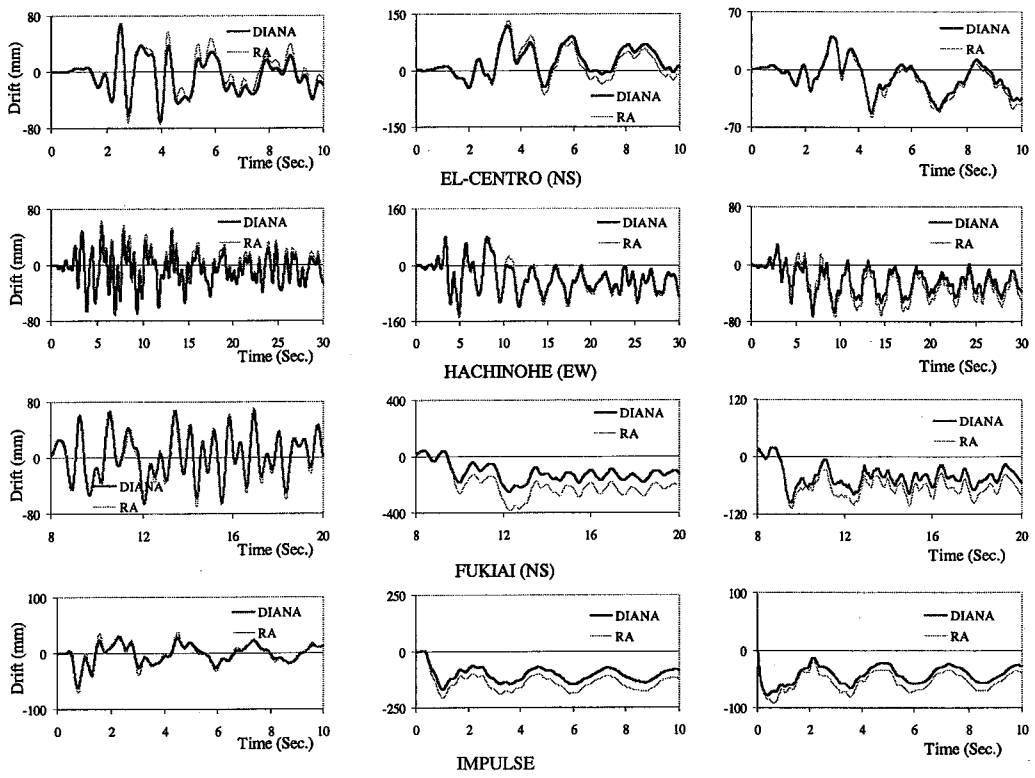

(a) Sixth Story Drift (b) Fifth Story Drift (c) First Story Drift

Fig. 12 Response History of Storey Drifts

3.2 Ellipsoidal yield surface of multi-story steel frames

(1) Ellipsoidal approximation of yield polyhedron of three-story frame

The safety domain against the plastic collapse of the multi-story frame is approximated as the n-dimensional hyper-ellipsoidal yield body, and a 3-story frame shown in Fig. 14(a) is studied. Pushover limit analysis is performed for this frame after the load pattern is determined as shown in Fig. 14(b). Furthermore the intersection of yield surface on the 1st and 2nd modal restoring force space is drawn in Fig. 14(c). Similarly, it is also considered that the number of mode is reduced before the limit analysis is performed. The results of the above-mentioned method are shown in Fig. 14(d), these show good agreements comparing to the exact yield polyhedron.

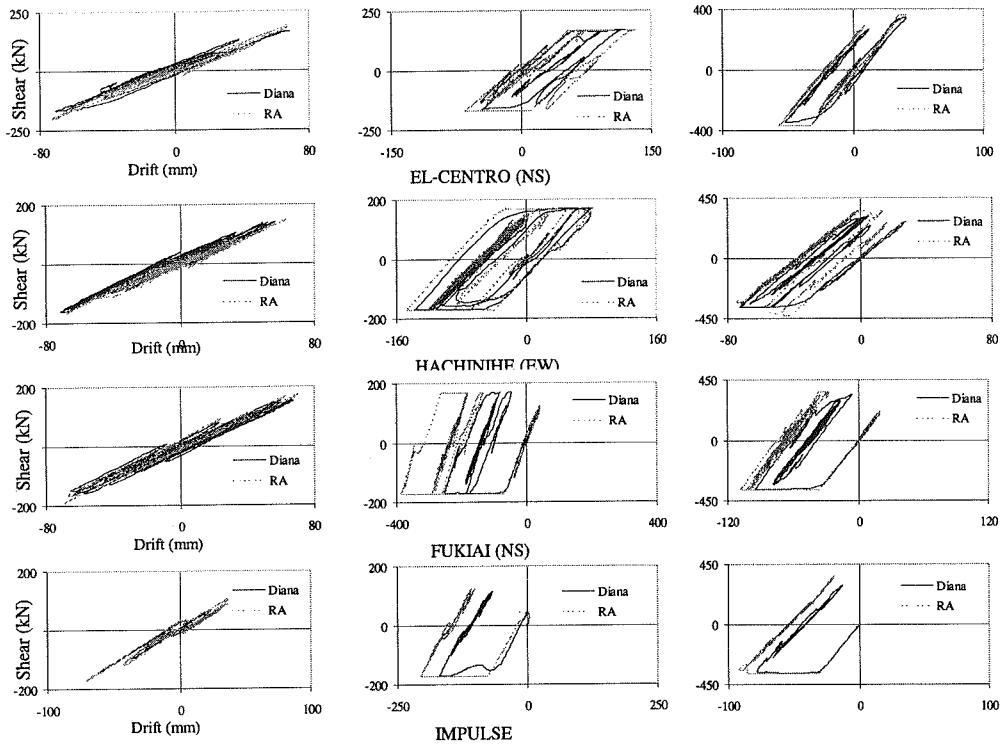

Fig. 13 Hysteresis Loops of Story Shear v/s Story Drift

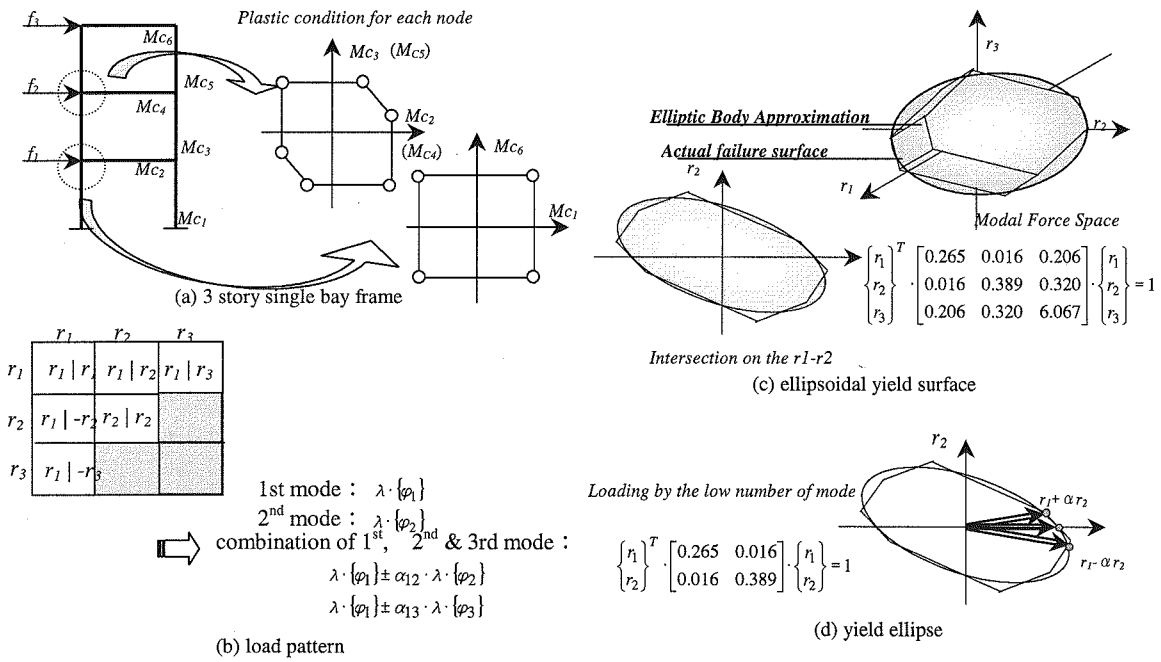

Fig. 14 Ellipsoidal approximation of yield surface of a three-story frame

(2) Full vibration-mode response analysis of two-story single-bay frame

An ellipsoidal body approximates the global safety domain against plastic mechanism formation of a frame, and a full or partial vibration-mode response analysis is performed. The results of response analysis and member-hysteresis based analysis are compared: The two-story single-bay frame in Fig. 3 is analyzed with full or (two) vibration-modes for El Centro NS 1940 320gal, and the following cases are studied for comparison:

1) Member-hysteresis based analysis, DIANA
2) Full mode response analysis with yield polyhedron model
3) Full mode response analysis with yield ellipse based on the pushover analysis

The time histories of story drift are shown in Fig. 15, and the loci of modal restoring force are shown in Fig. 16. The results of analyses based on simplified models show good chasing after the result of member hysteresis based analysis. And the locus of modal restoring force based on the yield ellipse approximated in case 3) looks very similar to the locus based on the exact yield polyhedron in case 2).

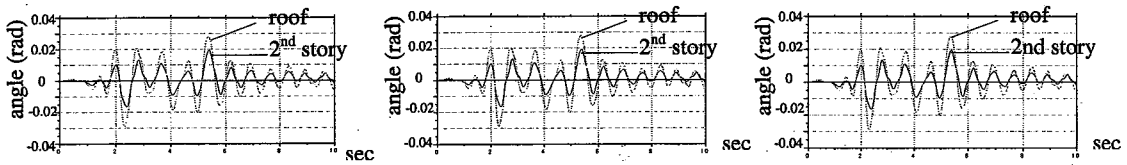

Member hysteresis based analysis　　full mode response analysis with yield polyhedron　　full mode response analysis with yield ellipse

Fig. 15 response history of story drift

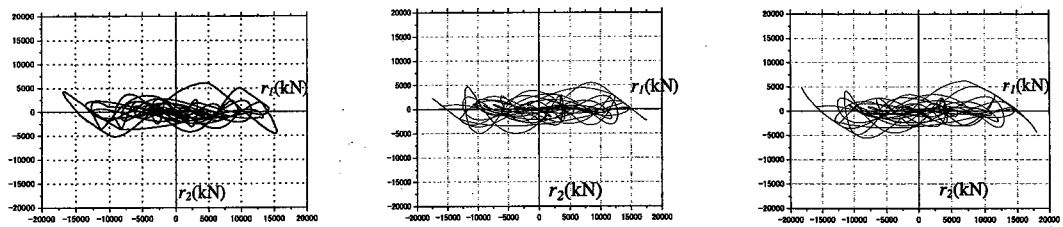

Member hysteresis based analysis　　full mode response analysis with yield polyhedron　　full mode response analysis with yield ellipse

Fig. 16 loci of modal restoring force

(3) Partial vibration-mode response analysis of six-story two-bay frame

The six-story two-bay frame in Fig. 7 is analyzed for El Centro NS 1940 320gal. Following three cases are studied:

1) Member hysteresis based analysis, DIANA
2) Partial vibration mode analysis (6DOF) with a yield polyhedron model with six relevant failure mechanisms
3) Partial vibration mode response analysis (2-DOF) with a yield ellipse model

The results of response history of story drift are shown in Fig. 17, the loci of modal restoring force are shown in Fig. 18. The maximum of drift in case 3) is large a little, however the partial mode response analysis with yield ellipse approximation has comparatively good chasing to member hysteresis based analysis in outline.

4. Conclusion

A simplified method of nonlinear dynamic response analysis on a moment-resisting steel frame to a seismic action is proposed: The method is based on two kinds of models for a safety domain against plastic collapse or a global yield surface of a frame: One is a yield polyhedron model with reduced number of failure mechanisms by the first-order

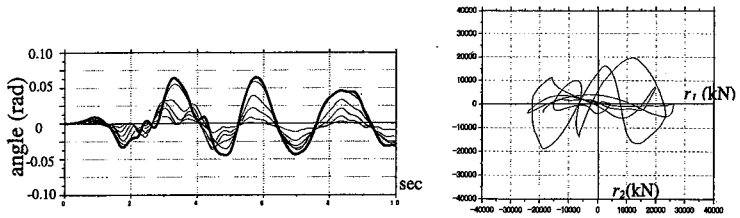

member hysteresis based analysis

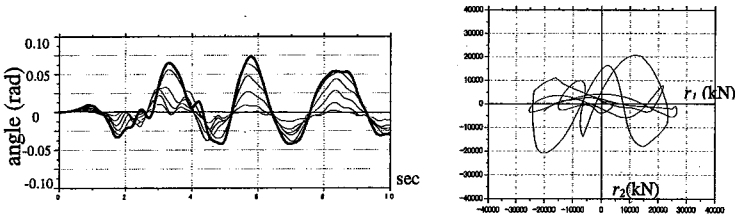

full mode response analysis with six-failure modes

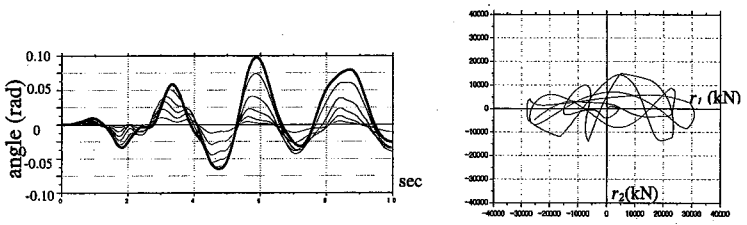

partial mode response analysis with yield ellipse

Fig. 17 response history of story drift Fig. 18 loci of modal restoring force

reliability method, and the other is a yield hyper-ellipsoidal model arranged to share some exact reference points on the yield surface obtained from pushover limit analysis. Either model is checked by comparison with detailed member hysteresis based analysis, and found to provide a consistently good prediction of global inelastic responses.

Reference

[1] FEMA, NEHRP Guidelines for the seismic rehabilitation of buildings, FEMA-273, Federal Energy Management Agency, USA, 1997

[2] Building Standard Law of Japan revised, 1998

[3] P.Khandelwal, Ohi.K, Fang.P, :"A Simple Proposal for Ultimate Seismic Demand Evaluation of Moment Resisting Steel Frames" , Journal of Structure and Construction Engineering, AIJ, Vol. 545, July, 2001

[4] Kenichi OHI, Peiyu FANG, and Praveen KHANDELWAL :"Dynamic Analysis with Reduced Modes by Yield Polyhedron Model for Steel Frames" , Journal of Construction Steel, Vol.8, pp.301-308, Nov. 2000

[5] Davenport, A.G., Note on the Distribution of the Largest Value of a Random Function with Application to Gust Loading, Proceedings of the Institution of Civil Engineers, Vol. 28, 1964, pp. 187-196

[6] Shibata, A., New Earthquake Resistant Structural Analysis, Morikita Press Co. Ltd., 1993, pp. 188-191 (In Japanese)

[7] Ang, A.H.S. and Tang, W.H., Probability Concepts in Engineering Planning and Design Volume II Decision, Risk and Reliability, John Wiley & Sons, pp. 504-506, 1984

[8] Ohi, K., Stochastic Limit Analysis of Framed Structures, Proc. of JCOSSAR' 91, pp. 675-678, JSCE, Nov. 1991 (In Japanese)

[9] Sun, H., Ohi, K. and Takanashi, K., A Proposal and Verification about Plastic Design Process with Target Collapse Mechanism for Structures, Proc. of 7th ICOSSAR, Nov. 1997.

[10] Dynamic Inelastic ANAlysis of steel frames, a private program coded by S.H. Gao and K.OHI, The University of Tokyo, 1987